Nanog-like Regulates Endoderm Formation through the Mxtx2-Nodal Pathway

Citation: Xu, Cong, Zi Peng Fan, Patrick Muller, Rachel Fogley, Anthony DiBiase, Eirini Trompouki, Juli Unternaehrer, et al. "Nanog-Like Regulates Endoderm Formation through the Mxtx2-Nodal Pathway." Developmental Cell 22, no. 3 (March 2012): 625–638. © 2012 Elsevier Inc.

As Published: http://dx.doi.org/10.1016/j.devcel.2012.01.003

Publisher: Elsevier

Persistent URL: http://hdl.handle.net/1721.1/91520

Version: Final published version: final published article, as it appeared in a journal, conference proceedings, or other formally published context

Developmental Cell
Article

Nanog-like Regulates Endoderm Formation through the Mxtx2-Nodal Pathway

Cong Xu,[1,2] Zi Peng Fan,[3] Patrick Müller,[4] Rachel Fogley,[1] Anthony DiBiase,[1,2] Eirini Trompouki,[1,2] Juli Unternaehrer,[1,2] Fengzhu Xiong,[5] Ingrid Torregroza,[6] Todd Evans,[6] Sean G. Megason,[5] George Q. Daley,[1,2] Alexander F. Schier,[4] Richard A. Young,[3] and Leonard I. Zon[1,2,*]
[1]Howard Hughes Medical Institute
[2]Division of Hematology/Oncology
Children's Hospital Boston and Dana-Farber Cancer Institute, Harvard Stem Cell Institute, Harvard Medical School, Boston, MA 02115, USA
[3]Whitehead Institute and Department of Biology, Massachusetts Institute of Technology, Cambridge, MA 02142, USA
[4]Department of Molecular and Cellular Biology, Harvard University, Cambridge, MA 02138, USA
[5]Department of Systems Biology, Harvard Medical School, Boston, MA 02115, USA
[6]Department of Surgery, Weill Cornell Medical College of Cornell University, New York, NY 10065, USA
*Correspondence: zon@enders.tch.harvard.edu
DOI 10.1016/j.devcel.2012.01.003

SUMMARY

In mammalian embryonic stem cells, the acquisition of pluripotency is dependent on Nanog, but the in vivo analysis of Nanog has been hampered by its requirement for early mouse development. In an effort to examine the role of Nanog in vivo, we identified a zebrafish Nanog ortholog and found that its knockdown impaired endoderm formation. Genome-wide transcription analysis revealed that *nanog-like* morphants fail to develop the extraembryonic yolk syncytial layer (YSL), which produces Nodal, required for endoderm induction. We examined the genes that were regulated by Nanog-like and identified the homeobox gene *mxtx2*, which is both necessary and sufficient for YSL induction. Chromatin immunoprecipitation assays and genetic studies indicated that Nanog-like directly activates *mxtx2*, which, in turn, specifies the YSL lineage by directly activating YSL genes. Our study identifies a Nanog-like-Mxtx2-Nodal pathway and establishes a role for Nanog-like in regulating the formation of the extraembryonic tissue required for endoderm induction.

INTRODUCTION

Pluripotency is defined as the capacity of a cell to give rise to all three germ layers. The homeobox gene *Nanog* was discovered on the basis of its ability to drive leukemia inhibitory factor (LIF) independent self-renewal of pluripotent mouse embryonic stem (ES) cells (Chambers et al., 2003; Mitsui et al., 2003). In ES cells, Nanog is a central player in the transcriptional regulatory circuitry of pluripotency (Boyer et al., 2005; Cole et al., 2008; Loh et al., 2006; Wang et al., 2006). In the early mouse embryo, *Nanog* expression marks the pluripotent epiblast and is essential for its establishment (Mitsui et al., 2003; Silva et al., 2009). A recent study has shown that activation of *Nanog* is required for acquisition of the pluripotent ground state in both embryonic development and somatic cell reprogramming (Silva et al., 2009). These studies raised the question of what function Nanog plays during embryonic development and prompted us to investigate this issue in the zebrafish model system.

The zebrafish blastula-stage embryo is composed of three distinct lineages: the extraembryonic enveloping layer (EVL), the extraembryonic yolk syncytial layer (YSL), and the intermediate deep cells, which form the entire embryo later. The YSL is unique to teleosts and has been thought to share a common evolutionary origin with the mouse extraembryonic primitive endoderm. Primitive endoderm markers such as *hex*, *gata6*, *gata4*, *pdgfra*, *hnf4a*, and *foxa3* are also expressed in the YSL (Brown et al., 2010; Fan et al., 2007; Ho et al., 1999; Sprague et al., 2006), and both tissues function as the signaling center to pattern the head mesoderm and endoderm (Chen and Kimelman, 2000; Fan et al., 2007; Ober and Schulte-Merker, 1999; Rodaway et al., 1999; Varlet et al., 1997). Between the 512 and 1K-cell stages, the collapse of marginal cells into the yolk cell results in the formation of the YSL precursor (Kimmel and Law, 1985b). Each YSL nucleus (YSN) undergoes usually three, but sometimes four or five, metasynchronous nuclear divisions and becomes postmitotic, just before the onset of epiboly (Kane et al., 1992; Kimmel and Law, 1985a). The YSL plays a critical role in producing the force to drive epiboly and inducing the ventrolateral mesoderm and endoderm (Chen and Kimelman, 2000; Mizuno et al., 1996; Ober and Schulte-Merker, 1999; Rodaway et al., 1999; Solnica-Krezel and Driever, 1994; Strähle and Jesuthasan, 1993).

During the midblastula stage, induction of endoderm requires the secreted Nodal proteins Ndr1 and Ndr2, which are expressed in the YSL and marginal blastomeres (Chen and Kimelman, 2000; Feldman et al., 1998; Ober and Schulte-Merker, 1999; Rodaway et al., 1999). In response, transcription of the endoderm transcription factors *gata5/faust*, *mixer/bon*, *mezzo*, and *sox32/cas* is induced in marginal blastomere cells (Dickmeis et al., 2001; Kikuchi et al., 2001, 2000; Poulain and Lepage, 2002; Reiter et al., 1999). Among them, *sox32/cas* plays a central role in endoderm induction, as its expression can autonomously induce the endodermal differentiation markers *sox17* and *foxA2* in the absence of Nodal signaling (Dickmeis et al., 2001; Kikuchi

et al., 2001). *sox32/cas* requires *pou5f1*, a ubiquitously expressed transcription factor, to maintain its expression and to activate *sox17* (Lunde et al., 2004; Reim et al., 2004).

In an effort to understand the role of Nanog in early zebrafish development, we identified the zebrafish *nanog* ortholog and found that it is required for YSL development. Knockdown of *nanog-like* eliminates ventrolateral Nodal signaling, resulting in an absence of ventrolateral endoderm formation. By microarray analysis, we found that *nanog-like* mophants do not express genes specific to the YSL, where Nodal signals are produced for endoderm induction. Genetic studies and chromatin immunoprecipitation-based sequencing (ChIP-Seq) analysis revealed that Nanog-like directly activates the transcription of the homeodomain factor Mxtx2, which, in turn, specifies the YSL and promotes ventrolateral endoderm formation. Our study illustrates a critical role for Nanog-like in regulating endoderm formation through the Mxtx2-Nodal pathway.

RESULTS

nanog-like Is Required for Early Gastrulation

To identify the zebrafish ortholog, we used the mouse Nanog protein sequence for a BLAST search. This approach resulted in the identification of Zgc:193933 as a potential zebrafish Nanog ortholog. The homology between mouse Nanog and zebrafish Zgc:193933 is evident in the homeodomain. Alignment of human, mouse, chicken, zebrafish, and medaka Nanog homeodomains showed high sequence conservation (Figure 1A). Furthermore, zebrafish, mouse, and human Nanog show a conserved intron/exon structure (Figure 1B). Significantly, in both fish and mammalian Nanog, the 60 amino acid (aa) homeodomain is encoded by the last 132 base pairs (bp) of the second exon and the first 48 bp of the third exon (Figure 1B). Such an intron/exon structure is not found in other closely related homeobox genes (Figure 1B; see also Figure S1A available online). No chromosomal synteny was present between the zebrafish and mammalian *Nanog* loci.

The zebrafish *nanog-like* cDNA was cloned from a blastula-stage embryo library and was used to examine gene expression by whole-mount in situ hybridization. *nanog-like* transcripts are maternally deposited (one-cell stage), expressed during the blastula stage (dome stage), and diminish rapidly during gastrulation (shield stage) (Figure 1C). At the end of gastrulation (tailbud stage), the transcripts can no longer be detected (Figure 1C).

To examine the role for Nanog-like in early embryogenesis, we knocked down the Nanog-like protein level using two distinct morpholinos targeting the *nanog-like* translational start site. Embryos injected with 10 ng of *nanog-like*-MO1 or 10 ng of *nanog-like*-MO2 at the one-cell stage exhibited similar gastrulation defects. The *nanog-like* knockdown blastomere showed slowed epibolic movement, resulting in the accumulation of blastomere cells at the animal pole at later stages (Figure 1D). When control morpholino-injected embryos reached the 80% epiboly stage, the majority of the *nanog-like* morphants (95 of 100) exhibited dramatic constriction of the marginal cells, causing the yolk cell to burst (Figure 1D). As shown by time-lapse microscopy of the *nanog-like*-MO2 injected embryo, the yolk burst process happened within 40 min (Figure 1E). To confirm that the gastrulation defects were specifically due to the knockdown of *nanog-like*, we injected 100 pg of *nanog-like* mRNA into the *nanog-like* morphant. The sequences at the *nanog-like* transcriptional start site were mutated to prevent hybridization with morpholinos. Phenotypes induced by both *nanog-like*-MO1 and *nanog-like*-MO2 were rescued by *nanog-like* mRNA (Figures 1F, 1G, and S1B). Notably, mRNA encoding human *NANOG* was also able to rescue the defects at a similar efficiency comparable to zebrafish *nanog-like* mRNA, confirming the evolutionary conservation between mammalian Nanog and zebrafish Nanog-like (Figures 1F, 1G, and S1B).

To test if Nanog-like functions in mouse ES cells, we examined whether mouse ES cells overexpressing *nanog-like* could self-renew in the absence of LIF. Previous studies have found that dimerization is required for Nanog to convey self-renewal in ES cells (Dixon et al., 2010; Wang et al., 2008). Examining the sequence outside of the homeodomain, we were unable to find the sequence for dimerization. To enable dimerization, Nanog-like was fused to the WR domain of mouse Nanog, which is required for dimerization (Figure S1D). By overexpressing engineered *nanog-like*, we were not able to rescue LIF dependence in ES cells (Figures S1E and S1F), despite findings that axolotl Nanog successfully rescues LIF dependence (Dixon et al., 2010). It seems that the zebrafish Nanog ortholog lacks the well-known self-renewal function that has been described in tetrapods. We therefore decided to name it Nanog-like.

Nanog-like Regulates Endoderm Formation by Activating Nodal

The most prominent defect observed in the *nanog-like* morphant is the impaired endoderm formation at the ventrolateral margin. The expression of endoderm genes *gata5*, *mixer*, *sox32*, and *sox17* is mostly restricted to the dorsal area in *nanog-like* morphants (Figure 2A). In zebrafish, endoderm formation is induced by high levels of Nodal, which activate *gata5/faust*, *mixer/bon*, and *mezzo* (Dickmeis et al., 2001; Feldman et al., 1998; Gritsman et al., 1999; Kikuchi et al., 2001, 2000; Poulain and Lepage, 2002; Reiter et al., 1999; Schier et al., 1997). These three transcription factors, in turn, control the expression of *sox32*. Sox32 cooperates with Pou5f1 to activate *sox17*, thereby specifying the endoderm lineage (Lunde et al., 2004; Reim et al., 2004). To determine if the lack of endoderm cells at the lateral and ventral margin was due to reduced Nodal signaling, we examined the expression of Nodal genes *ndr1* and *ndr2*. At the sphere stage, *ndr1* and *ndr2* expression was normal at the dorsal margin in the *nanog-like* morphant (data not shown) but failed to spread to the ventrolateral area at the dome stage (Figure 2B). This defect is specifically due to the knockdown of *nanog-like*, as ventrolateral *ndr1* and *ndr2* expression can be rescued by restoring *nanog-like* mRNA (Figure 2B). Ventrolateral *ndr1* and *mixer* expression was evident in some *nanog-like* morphants at the 50% epiboly stage (data not shown). To confirm that the ventrolateral endoderm defect was due to a lack of local Nodal signaling, we injected *ndr1* mRNA into the vegetal yolk of the four-cell-stage embryo. This approach allowed the targeting of the YSL and marginal cells with *ndr1* mRNA (Figures S2A and S2B). As expected, *ndr1* expression restored the ventrolateral endoderm markers in the *nanog-like* morphant (Figure 2C).

Since the ventrolateral expression of *ndr1* and *ndr2* is dependent on activated Nodal signaling by an autoregulatory feedback,

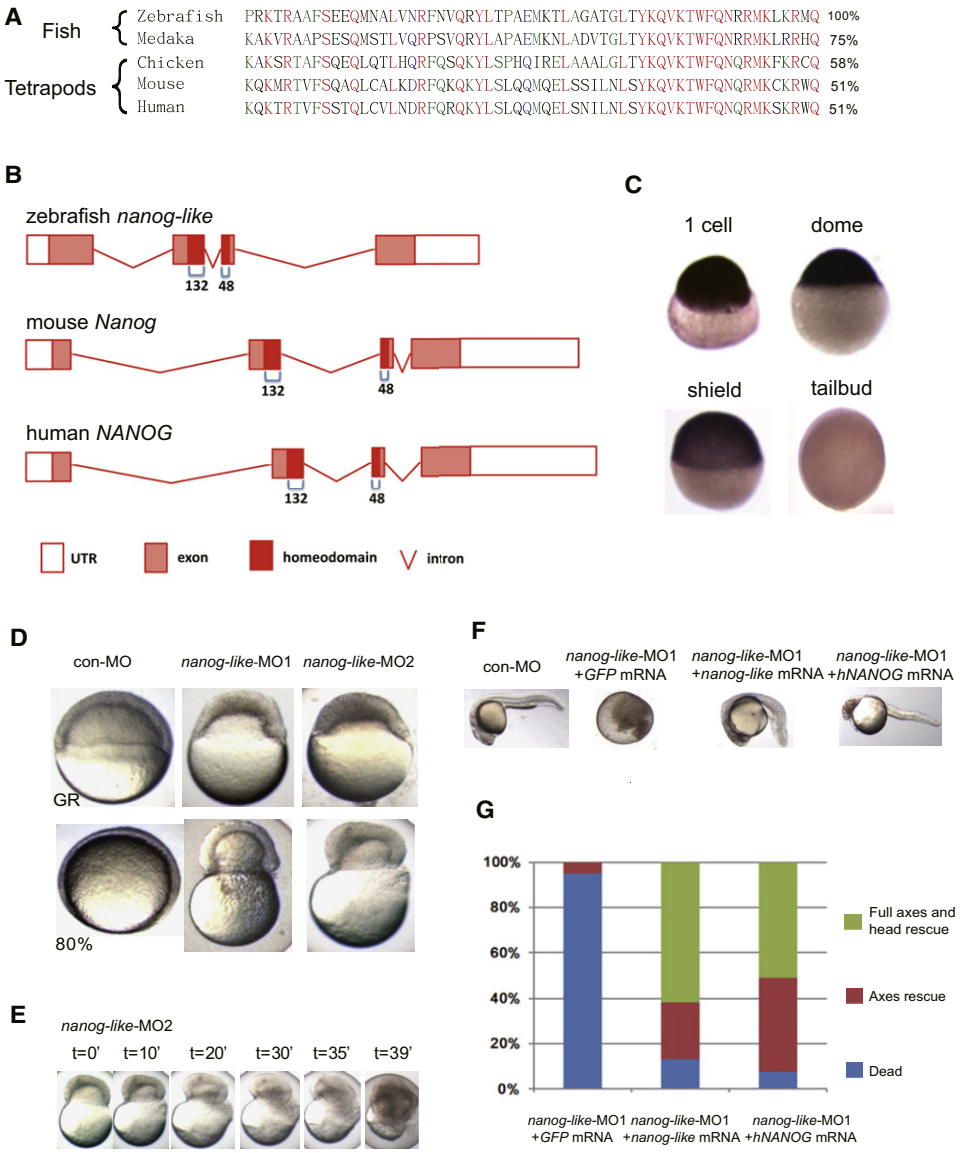

Figure 1. Identification of the Zebrafish *nanog-like* Gene

(A) Alignment of the homeodomain sequence of fish and tetrapod Nanog proteins. The percentage similarity of each to zebrafish Nanog-like is shown at the right.

(B) Intron/exon structure of the zebrafish, mouse, and human *Nanog* genes. The 60-aa homeodomain is encoded by the last 132 bp of the second exon and the first 48 bp of the third exon in all three organisms.

(C) Whole-mount in situ hybridization of *nanog-like* identified high maternal (1-cell) and blastula (dome) expression, and rapidly diminishing expression during gastrulation (shield and tailbud stages).

(D) Blastomeres of *nanog-like*-knockdown embryos, injected with one of two distinct morpholinos targeting the translational start site, failed to thin at the germ ring stage and constricted to squeeze out the yolk cell by the 80% epiboly stage.

(E) Time-lapse microscopy of the *nanog-like*-MO2-injected embryo showing the yolk burst process.

(F) Rescue of the *nanog-like*-MO1-injected embryos by coinjection of 100 pg zebrafish *nanog-like* or human *NANOG* mRNA. Embryos shown are at 24 hpf.

(G) Statistics for the rescue of *nanog-like*-MO1-injected embryos by zebrafish *nanog-like* or human *NANOG* mRNA. A total of 100 *GFP* mRNA-injected, 115 *nanog-like* mRNA-injected, and 209 human *NANOG* mRNA-injected embryos were analyzed. Phenotype classes were counted at 24 hpf and are presented as a percentage of the whole.

the absence of ventrolateral Nodal expression in *nanog-like* morphants might be due to the inability of cells to induce *ndr1* and *ndr2* expression on receiving Nodal signals. To test this possibility, we activated the Nodal pathway by expressing the constitutively active Nodal receptor *Tar**. *ndr1* and *ndr2* expression can be induced in *Tar** expressing *nanog-like* morphants, indicating that the lack of ventrolateral Nodal expression is not due to a modulated competence for Nodal autoregulation (Figure S2C).

Nanog-like Regulates YSL Transcription

The yolk burst phenotype seen in the *nanog-like* morphant is unlikely due to the endoderm defect, as endoderm mutants

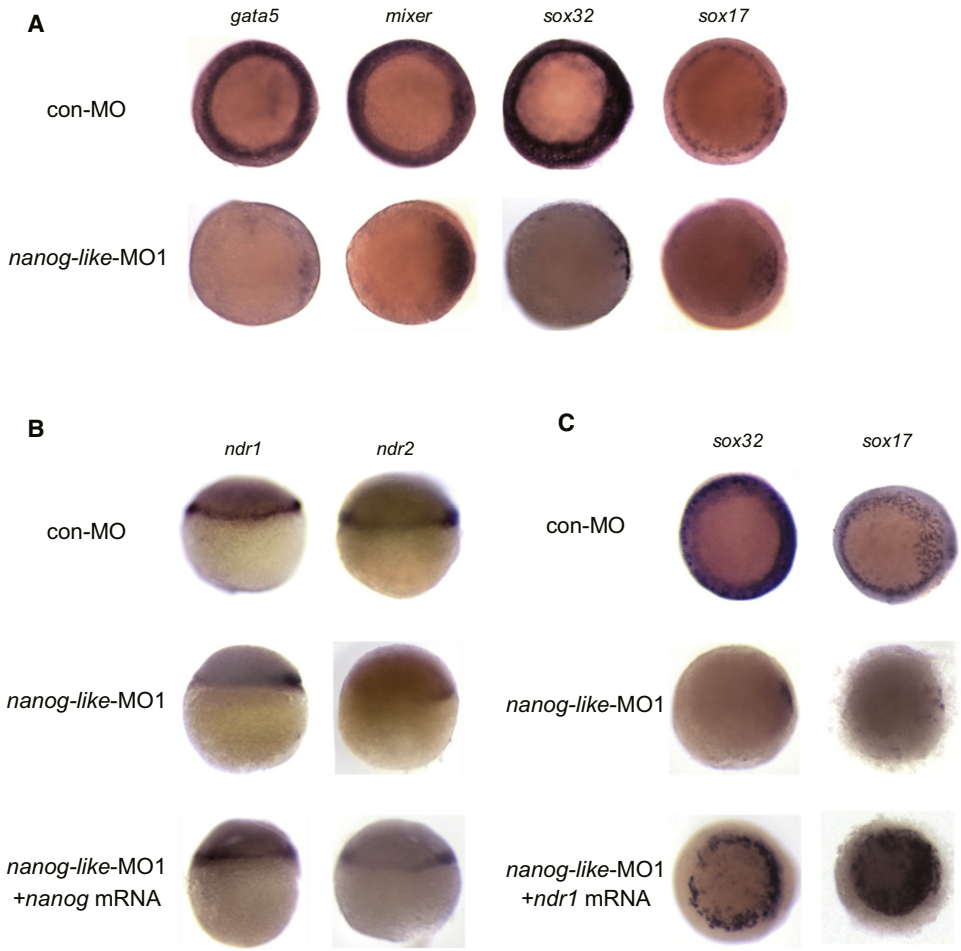

Figure 2. Nanog-like Regulates Endoderm Formation by Activating Nodal

(A) *nanog-like* knockdown impairs ventrolateral endoderm formation. The endoderm genes *mixer*, *gata5*, *sox32*, and *sox17* are absent at the ventrolateral margin in *nanog-like*-MO1-injected embryos. All views are shown as an animal view with the dorsal side to the right.

(B) *ndr1* and *ndr2* expression is restricted to the dorsal area in the *nanog-like*-MO1-injected embryo; ventrolateral expression of both genes can be restored by coinjection of *nanog-like* mRNA. All views are lateral with the presumptive dorsal side to the right.

(C) Ventrolateral *sox32* and *sox17* expression can be rescued by *ndr1* mRNA. All views are shown as an animal view with the presumptive dorsal side to the right.

undergo epiboly without constricting the yolk (Dickmeis et al., 2001; Feldman et al., 1998; Gritsman et al., 1999; Kikuchi et al., 2001; Schier et al., 1997). To globally analyze which target genes Nanog-like regulates during early embryogenesis, we performed a genome-wide transcription analysis using sphere stage (4 hr postfertilization [hpf]) *nanog-like* morphants. We identified Nanog-like regulated genes by a q value smaller than 0.01 in three separate experiments. Nanog-like regulates a discrete set of genes (609 in total, 362 upregulated and 247 downregulated). Genome-wide ontology analysis revealed that both upregulated and downregulated genes are enriched for the role of Nanog in mammalian embryonic stem cell pluripotency (Figures S3A and S3B). Among the top downregulated genes, we noticed a group of genes that are expressed exclusively in the YSL, suggesting a YSL defect in *nanog-like* morphants (Figure 3A). We further verified the decreased YSL gene expression in sphere-stage and 50%-epiboly-stage embryos by RT-PCR (Figure S3C) and in situ hybridization (Figure 3B; Figure S4A).

The YSL forms at 2.5 hpf, when the marginal cells collapse into the yolk cell to form a multinucleated syncytium. To examine if the YSL formed correctly in the *nanog-like* morphant, we injected the vital dye SYTOX into the yolk cell of 1K-cell-stage embryos to visualize the YSN. YSN in *nanog-like* morphants were present at the ring area, indicating that the syncytial structure formed correctly (Figure 3C). However, at the 50% epiboly stage, we observed decreased YSN number in the *nanog-like* morphant (Figure 3C). To visualize the division and movement of YSNs, we performed time-lapse confocal microscopy (Movies S1 and S2). Both wild-type and morphant embryos undergo the 12th division, but some YSNs in the morphant fail to separate completely (Figure 3D; Movie S2). During and after the 12th division, aggregation of YSNs is evident in the morphant (Figure 3D; Movie S2). Imaging of the aggregated YSNs under higher resolution shows that they stack together with clear nuclear boundaries, suggesting that the decrease in YSN number is due only to the aggregation of YSNs (Figure 3E).

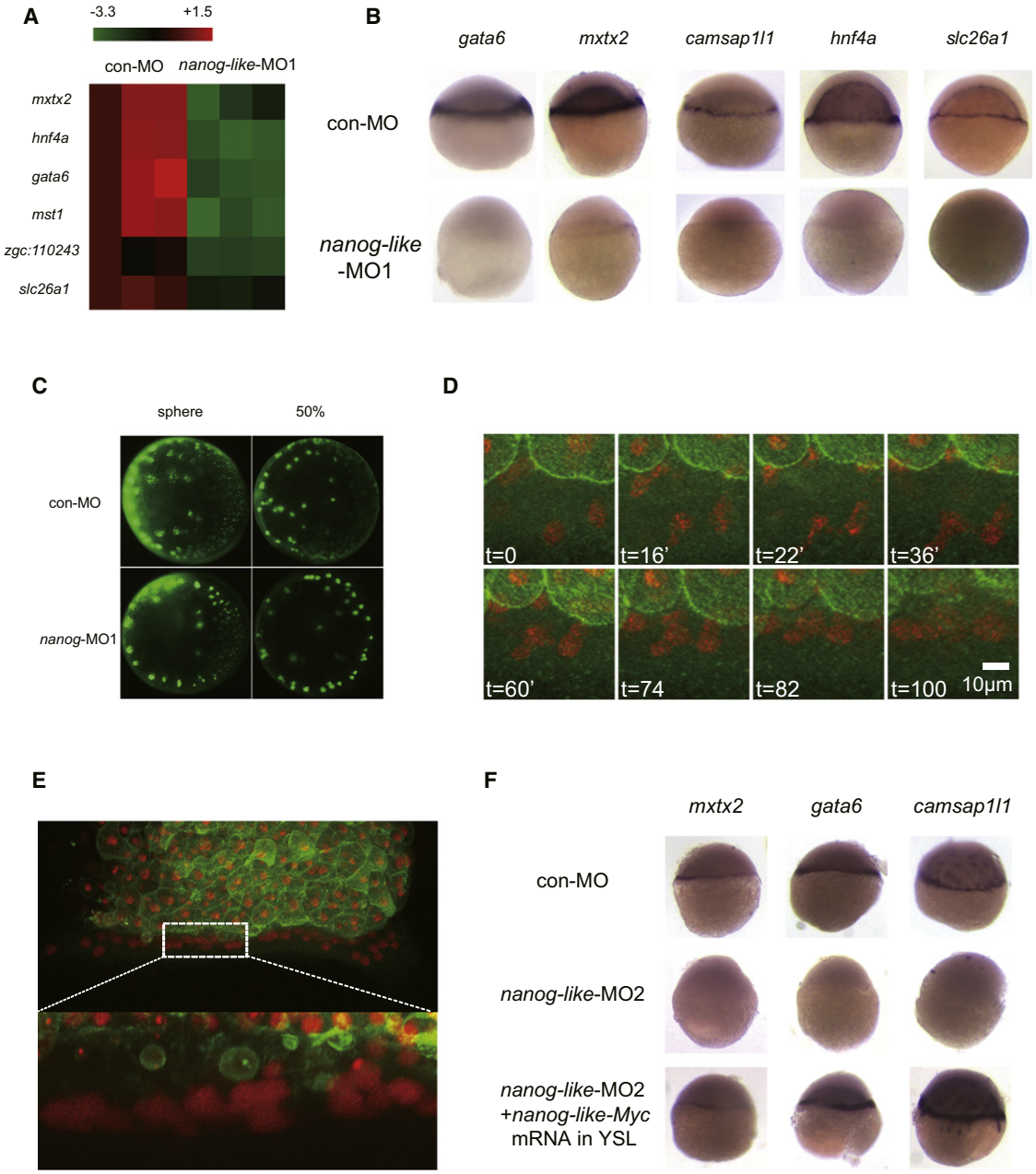

Figure 3. Lack of YSL Transcription in *nanog-like* Morphants Leads to Epiboly and Endoderm Defects

(A) Microarray analysis of gene expression in *nanog-like* morphants revealed an absence of YSL gene transcription. YSL genes downregulated in three separate experiments are displayed as a heat map.

(B) The expression of *gata6*, *mxtx2*, *camsap1l1*, *hnf4a*, and *slc26a1* is absent in the YSL of *nanog-like* morphants. All views are lateral with the presumptive dorsal side to the right.

(C) The YSN of the wild-type and *nanog-like* knockdown embryos at the sphere stage and the 50% epiboly stage labeled with SYTOX green. All views are shown as an animal view with the dorsal side to the right.

(D) Time-lapse microscopy of the YSNs of a *nanog-like*-MO2-injected embryo revealed the YSN aggregation process. Three YSNs undergo the 12th division at t = 16 min. At t = 22 min, the upper left YSNs separate normally while the lower YSNs fail to completely separate. At t = 36 min, the resulting six daughter YSNs start to aggregate.

(E) Higher magnitude confocal microscopy revealed that the aggregated YSNs in Figure 3D remained separated.

(F) Nanog-like is required autonomously for YSL transcription. To achieve YSL-specific expression, 300 pg *nanog-like-Myc* mRNA was injected into the yolk at 2.5 hpf. The expression of *mxtx2*, *gata6*, and *camsap1l1* was rescued by YSL-specific *nanog-like-Myc* expression.

Fusion of YSNs was not observed in the time-lapse movies (Movies S1 and S2).

Active remodeling of cytoskeletal filaments at the YSL-EVL junction provides force for vegetal movement of the blastoderm. Within the YSL is an F-actin band, which is considered critical for epiboly movement (Cheng et al., 2004; Köppen et al., 2006). Rhodamine-labeled phalloidin staining showed that no detectable F-actin band formed in *nanog-like* morphants (Figure S4B). We postulate that the absence of F-actin band might be due to the defective YSL transcription in *nanog-like* morphants.

Lack of YSL Transcription Leads to the Epiboly and Endoderm Defects

To examine the effect of defective YSL transcription, we injected RNase into the yolk cell of the wild-type 1K-cell-stage embryo. Previous studies showed that this approach ablates the RNA transcripts, specifically in the YSL, without affecting protein stability (Chen and Kimelman, 2000). Consistent with the previous report (Chen and Kimelman, 2000), we noticed that injected embryos showed slowed epiboly movements followed by a yolk burst at the shield stage, phenocopying the defects seen in *nanog-like* morphants (data not shown). Previous study showed that the YSL transcripts are required for ventrolateral mesoendoderm induction (Chen and Kimelman, 2000). We re-examined the Nodal signals and endoderm lineage and found that the Nodal genes *ndr1* and *ndr2* and the endoderm gene *mixer* were absent in the ventrolateral area (data not shown). All of these data suggested that the lack of YSL gene expression in the *nanog-like* morphant was responsible for the epiboly and endoderm defects.

To confirm that the epiboly defect in *nanog-like* morphants was due to defective YSL formation, we generated chimeric embryos by exchanging blastoderm and YSL tissues between wild-type and *nanog-like* knockdown embryos at the 1K-cell stage. Chimeric embryos with a wild-type YSL and a *nanog-like* morphant blastoderm were able to fully undergo epiboly and survived to 3 days postfertilization (dpf) (data not shown). In contrast, chimeric embryos with a *nanog-like* knockdown YSL and a wild-type blastoderm failed to initiate epiboly, resulting in the accumulation of wild-type blastomere cells at the animal pole (data not shown). As a complementary approach to address the YSL-autonomous requirement for Nanog-like, we knocked down Nanog-like in the whole embryo and restored its YSL expression by injecting *nanog-like-Myc* mRNA into the yolk after YSL formation, a method employed to achieve YSL-specific expression (Figure S4C). Expression of *mxtx2*, *gata6*, *camsap1l1*, and *hnf4a* was rescued by YSL-specific expression of *nanog-like-Myc* (Figure 3E; data not shown), suggesting that Nanog-like regulates YSL transcription in a cell-autonomous manner. These results indicate that the YSL is critical for epiboly movements and that Nanog-like regulates transcription in the YSL to promote both epiboly and endoderm development.

Nanog-like Controls the Expression of *mxtx2*, a Homeodomain Factor Required for and Sufficient for YSL Induction

As Nanog-like alone cannot induce YSL, we were interested in identifying the key mediators downstream of Nanog-like that regulate the proper formation and function of YSL. One candidate downregulated in the *nanog-like* morphants is *mxtx2,* a homeobox gene that is among the earliest genes known to be expressed in the YSL (Bruce et al., 2005; Wilkins et al., 2008), *mxtx2* transcription is induced by stabilized β-catenin shortly after the midblastula transition in the dorsal area and can be detected in the marginal blastoderm and the YSL at later stages. Knockdown of *mxtx2* leads to a yolk burst phenotype similar to that observed in the *nanog-like* morphant (Figure 4A) and (Wilkins et al., 2008). In *nanog-like* morphants, *mxtx2* expression is initiated in the dorsal area but fails to spread to ventrolateral regions, suggesting that *mxtx2* expression consists of Nanog-like-dependent ventrolateral and Nanog-like-independent dorsal expression (Figure 3B; data not shown).

To further characterize the role of Mxtx2 in YSL development, we examined the expression of YSL genes in *mxtx2* morphants. Notably, all YSL genes examined were absent in *mxtx2* morphants (Figure 4A). Conversely, embryos overexpressing *mxtx2* in blastomeres showed severe gastrulation defects and ectopic expression of YSL genes (Figure 4A). We also found that Nodal signaling and endoderm formation were compromised in the *mxtx2* morphant. *ndr1* is expressed in the ventrolateral margin with delayed onset (Figure 4B; data not shown). Expression of *ndr2* and endodermal genes was impaired at the ventrolateral margin (Figure 4B). Individual *gata5*- and *sox32*-positive cells were sparsely present at the ventrolateral margin (Figure 4B; data not shown), which were presumably induced by residual Ndr1. A recent study by Hong et al. (2011) also found that Mxtx2 directly activates *ndr2* in the YSL. Our study reveals a role for Mxtx2 in the induction of YSL gene transcription beyond *ndr2*.

To determine if *mxtx2* is the direct target of Nanog-like, we used cycloheximide (CHX) at 2 hpf to block translation of the earliest zygotic transcripts but allow the translation of injected *nanog-like-Myc* mRNA. When CHX is added at 2 hpf, expression of *mxtx2*—but not *gata6*, *camsap1l1*, or *hnf4a*—can be rescued in *nanog-like* morphants, indicating that *mxtx2* is the direct target of Nanog-like (Figure 4C; data not shown).

Genome-wide Association of Nanog-like Binding with Expression Profile of the *nanog-like* Morphant

To determine the downstream targets of Nanog-like and Mxtx2, we performed ChIP-Seq analysis on blastula embryos. The 3′ end of the *nanog-like* coding sequence was fused to a *Myc* tag sequence. *nanog-like-Myc* mRNA rescued *nanog-like* morphants at a similar efficiency as *nanog-like* mRNA (Figure S1C). Wild-type embryos were injected with *nanog-like-Myc* mRNA at a dosage (25 pg/embryo) that did not cause any developmental abnormality and were collected for ChIP-Seq analysis at the high (3.3 hpf) or dome (4.3 hpf) stage. We found that Nanog-like bound to many known mouse Nanog targets like *pou5f1*, *nanog-like*, and *sox2* (Figure 5A). In an effort to determine if zebrafish and mice share similar Nanog targets, we compared our targets with two previous studies in mouse ES cells and found that zebrafish Nanog-like targets are highly enriched in mouse targets from both studies, suggesting evolutionary conservation of the transcription network (Figure 5B) (Chen et al., 2008; Marson et al., 2008).

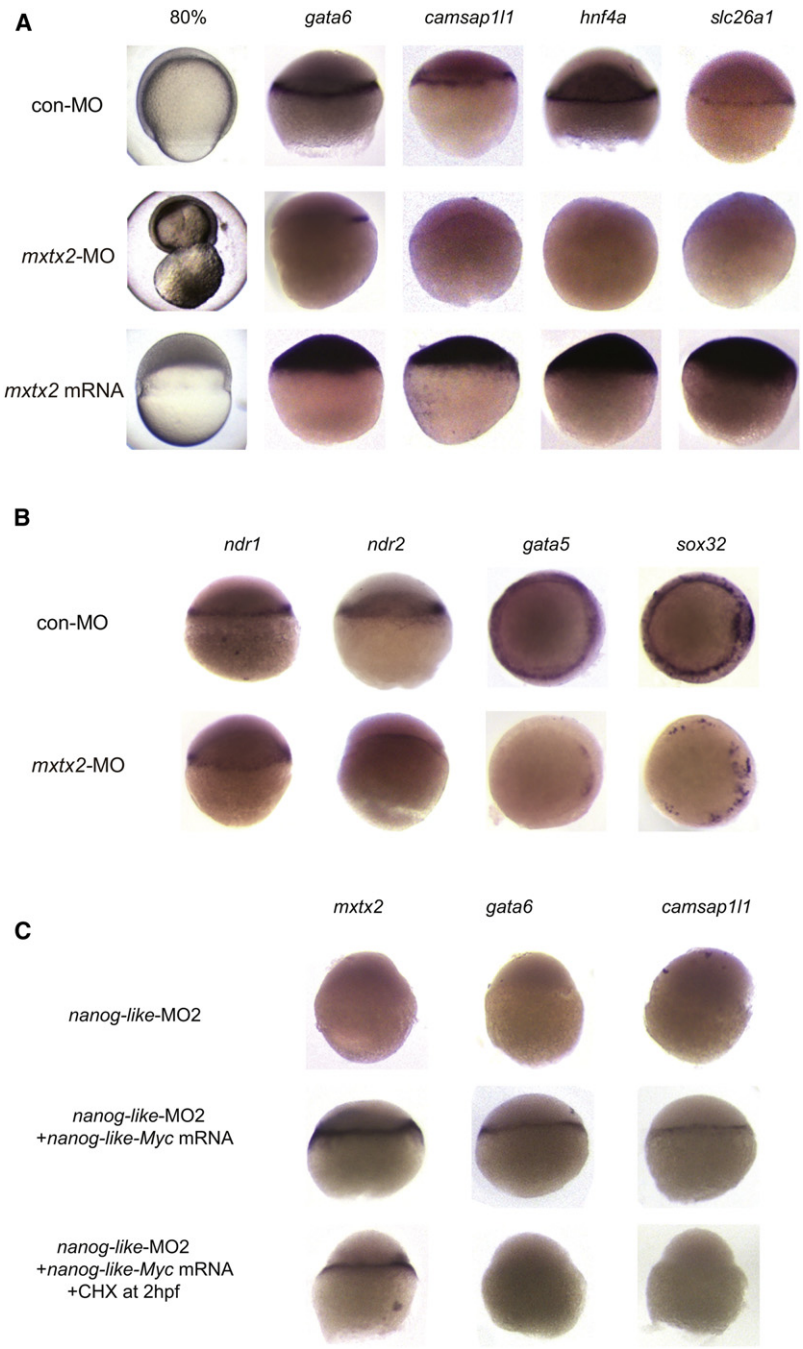

Figure 4. Mxtx2 Is Required for and Sufficient for YSL Induction

(A) Lateral view of embryos injected with 500 pg control morpholino (con-MO), 500 pg *mxtx2* morpholino (*mxtx2*-MO), or 100 pg *mxtx2* mRNA at the one-cell stage. At the 80% epiboly stage, *mxtx2* morphants develop a yolk burst phenotype, and the *mxtx2* mRNA-injected embryo failed to undergo epiboly. The YSL markers *gata6*, *camsap1l1*, *hnf4a*, and *slc26a1* were absent in the *mxtx2* morphant. YSL genes were ectopically expressed in the embryos injected with *mxtx2* mRNA.

(B) Defective Nodal signaling and endoderm formation in the *mxtx2* morphant. *ndr1* and *ndr2* are shown as a lateral view with the presumptive dorsal side to the right. *gata5* and *sox32* staining is shown as an animal view with the dorsal side to the right.

(C) By overexpressing *nanog-like-Myc*, expression of *mxtx2*, *gata6*, and *camsap1l1* in *nanog-like* morphants can be rescued. CHX was added at 2 hpf to allow for the translation of injected *nanog-like-Myc* mRNA but to prevent translation of the earliest zygotic transcripts. When CHX is added at 2 hpf, expression of *mxtx2*, but not *gata6* or *camsap1l1*, can still be rescued, indicating that *mxtx2* is the direct target of Nanog-like.

Overall, we identified 11,344 regions bound at the high stage and 14,010 regions bound at the dome stage. This correlated to 3,577 genes bound at the high stage and 4,595 genes bound at the dome stage. Nanog-like binding profiles between the two stages were similar, indicated by a large number of co-occupied regions (6,108) and colocalization heat map analysis (Figures 5C and 5D). For each developmental stage, we performed de novo motif analysis and found similar motifs to the previously reported mouse Nanog binding motifs (Figure 5C) (Chen et al., 2008; Loh et al., 2006). To associate the binding data with the microarray data, we examined the downregulated genes from microarray analysis and their binding frequency and found that the top 100 downregulated genes are highly enriched for Nanog-like binding (Figure 5E).

To analyze how Nanog-like regulates *mxtx2* expression, we examined Nanog-like's binding profile at the *mxtx2* locus. The binding of Nanog-like at the *mxtx2* locus is dynamic. At the high stage, Nanog-like binding covers the entire coding region. Notably, as indicated by the total target counts, the binding at the *mxtx2* locus is the strongest across the entire genome, suggesting a particularly available locus for selective binding by Nanog-like. At the dome stage, binding is distributed to distinct peaks at the promoter, in the gene, and downstream regions (Figure 5A), and the peak height is lower than the one at the high stage.

Mxtx2 Directly Binds Genes Expressed in YSL

To determine whether YSL genes are direct Mxtx2 targets, we performed ChIP-Seq analysis on *mxtx2-Myc* mRNA-injected embryos at the dome stage. The 3′ end of the *mxtx2* coding sequence was fused to a *Myc* tag repeat sequence. To determine if the fused Mxtx2-Myc protein was physiologically functional, we injected the *mxtx2-Myc* mRNA into one-cell stage embryos and found that it was capable of inducing ectopic YSL gene expression (Figure S5A). We examined all of the 12 YSL genes published by Hong et al. (Hong et al., 2010) and found that 11 of the 12 were bound by Mxtx2 (Figure 6A; Figure S5B). We also found that *ndr1* and *ndr2* were bound by Mxtx2, suggesting a direct activation of Nodal genes by Mxtx2 (Figure 6A). We expanded this analysis further by generating a YSL gene list containing all

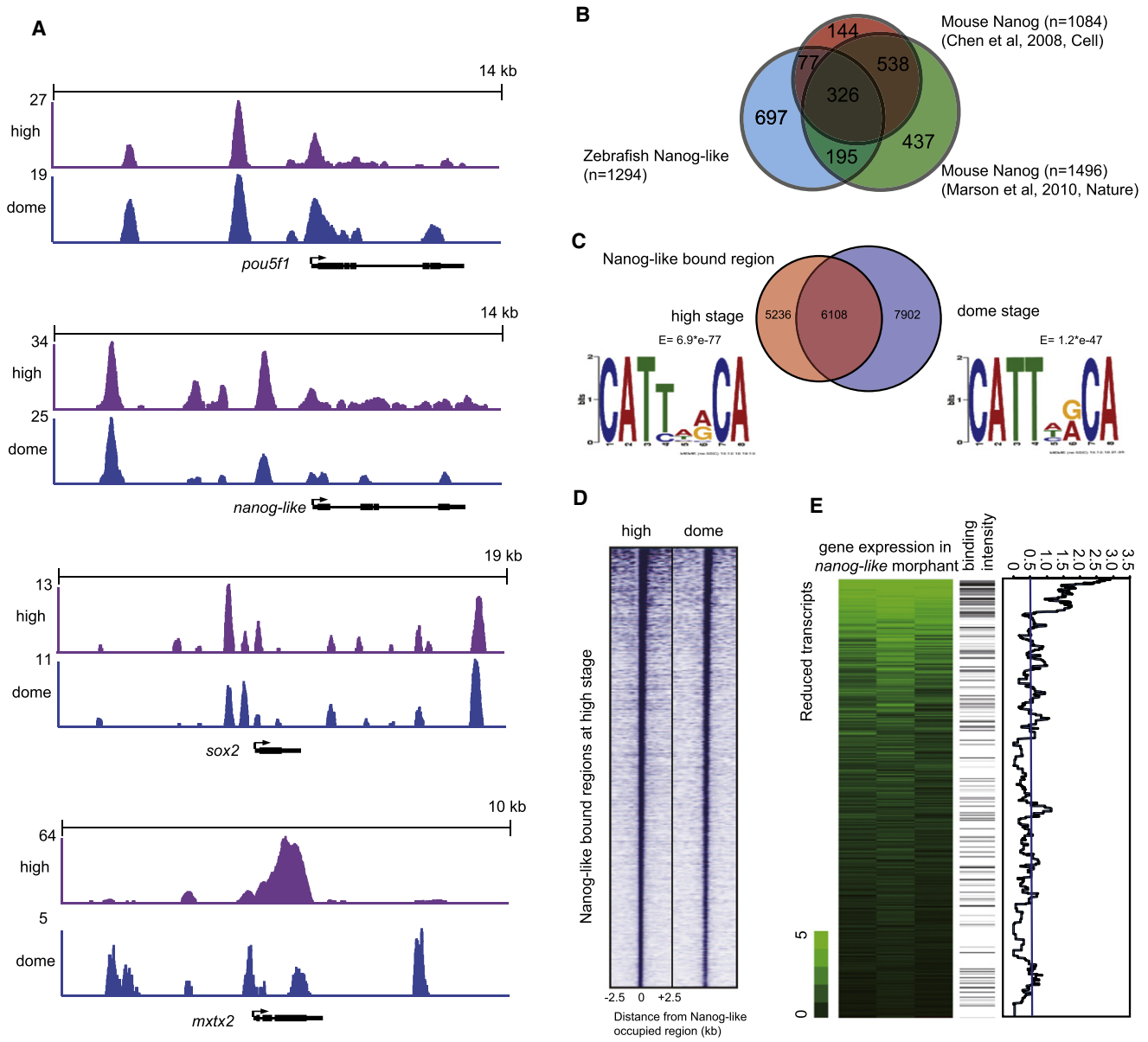

Figure 5. Genome-wide Association of Nanog-like Binding with the Expression Profile of *nanog-like* Morphants

(A) Nanog-like binding profiles at *pou5f1*, *nanog-like*, *sox2*, and *mxtx2* loci. ChIP-Seq data are shown in reads per million, with the *y* axis floor set to 2 reads per million.

(B) We generated a list with 4,736 genes that can be identified in both zebrafish and mice. We restricted our comparison of Nanog targets to these genes. The Venn diagram shows the overlap among zebrafish Nanog-like targets and two previously reported mouse Nanog targets (Chen et al., 2008; Marson et al., 2008). By the hypergeometric test, we found that zebrafish Nanog-like targets are enriched in both Chen's ($p = 3e\text{-}16$) and Marson's ($p = 3e\text{-}15$) mouse Nanog targets.

(C) Venn diagram indicating the number of sites bound by Nanog-like at the high or dome stage ($p < e^{-15}$). For each occupancy data set, the de novo binding motif is indicated.

(D) Region map showing that Nanog-like binding sites at the high and dome stages colocalize. For each Nanog-like occupied region at the high stage, the occupancy of dome-stage Nanog-like is indicated within a 5 kb window centered on the high-stage Nanog-like region.

(E) Left: Transcripts reduced in *nanog-like* morphants detected in triplicate samples by a ratio relative to controls. Middle: Nanog-like binding frequency within 100 kb of the corresponding genes, indicated by intensity of black shading. Binding is observed more frequently near loci with reduced expression, suggesting direct regulation of many top downregulated targets. Right: moving average of the Nanog-like binding intensity. The average binding intensity of 0.52 is derived from the ratio of the sum of Nanog-like binding frequency over the total number of genes interrogated (vertical blue line).

271 genes having expression in the YSL during gastrulation (Table S3B) based on expression patterns in ZFIN (Sprague et al., 2006). We found 11.3% of the genes (1,751 of all annotated 15,500 zebrafish genes) and 43.6% of the YSL genes (118 of 271 genes expressed in the YSL) were bound by Mxtx2 (Figure 6C). The bound genes are highly enriched for YSL genes, as indicated

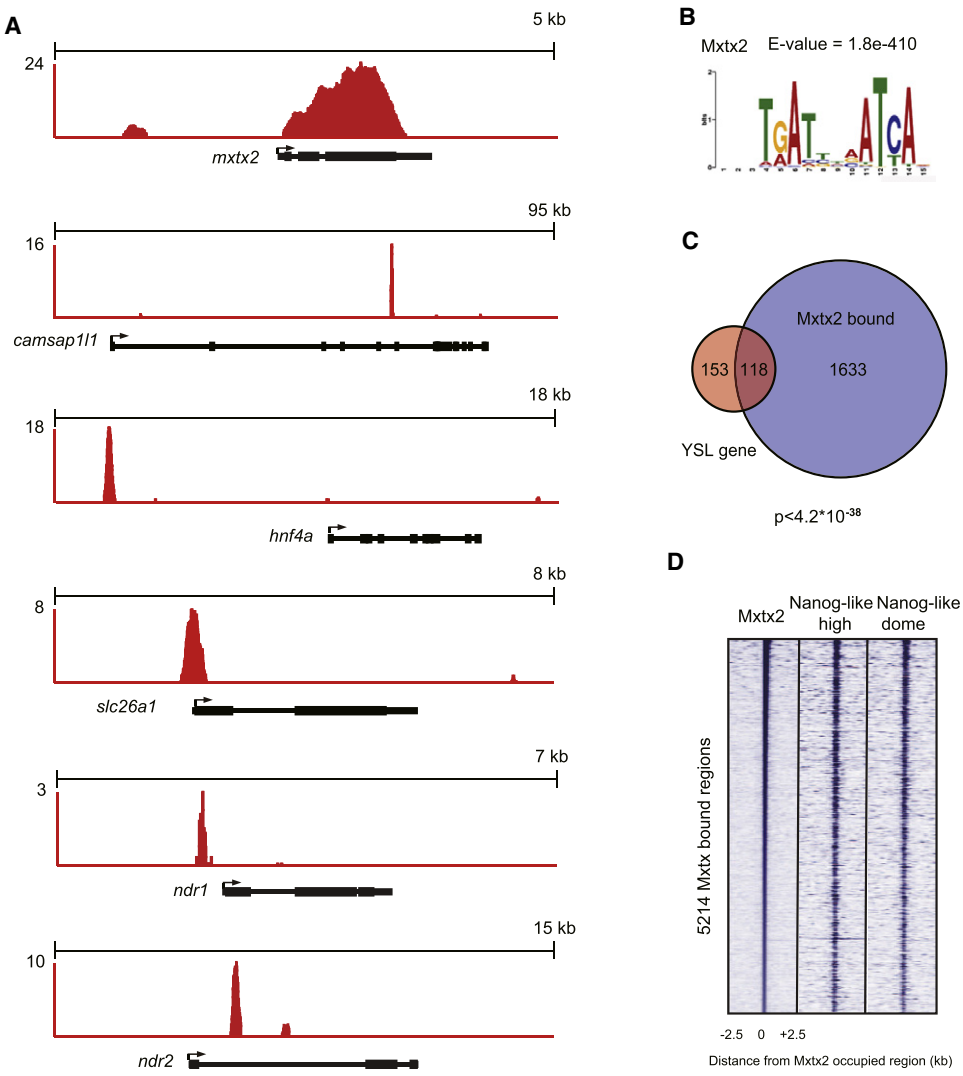

Figure 6. Mxtx2 Directly Binds Genes Expressed in YSL

(A) Mxtx2 binding profiles at *mxtx2*, *camsap1l1*, *hnf4a*, *slc26a1*, *ndr1*, and *ndr2* loci. ChIP-Seq data are shown in reads per million with the *y* axis floor set to two reads per million.

(B) de novo prediction of the Mxtx2 binding motif, utilizing sequences of the top 1,000 Mxtx2 binding regions.

(C) Venn diagram showing the overlap of high-confidence ($p < 10^{-9}$) Mxtx2-occupied sites with genes expressed in the YSL. The hypergeometric test suggests that the Mxtx2-bound genes are highly enriched for known YSL genes ($p < 4.2 \times 10^{-38}$).

(D) Region map showing that Mxtx2 and Nanog-like colocalize at many Mxtx2-bound sites. For each Mxtx2-occupied region, the occupancy of Nanog-like is indicated within a 5 kb window centered on the Mxtx2-bound region.

by the hypergeometric test ($p < 4.2 \times 10^{-38}$). We performed de novo motif analysis and identified a palindromic Mxtx2 binding motif, which suggested that dimerization of Mxtx2 may be required for DNA binding (Figure 6B). We noticed that many of the Mxtx2 binding loci were also occupied by Nanog-like (Figure S5C). This includes the presence of Nanog-like and Mxtx2 binding at the *nanog-like* and *mxtx2* loci, potentially allowing for cross-regulation and autoregulation of these genes.

Mxtx2 Rescues Defects in the *nanog-like* Morphant

To test if the *nanog-like* morphant phenotype could be rescued by restoring Mxtx2, we coinjected *mxtx2* mRNA and *Green Fluorescent Protein* (*GFP*) mRNA into the yolk of the four-cell stage *nanog-like* morphant and collected embryos with *GFP* expression in the YSL for further analysis. We examined different YSL markers and found that Mxtx2 restored the YSL lineage in the *nanog-like* morphant (Figure 7A). We further examined whether gastrulation defects could be rescued by Mxtx2. Among the 78 *mxtx2*-injected *nanog-like* morphants, 35 exhibited normal epiboly at the 80% epiboly stage, suggesting that the yolk burst phenotype was, at least in part, due to a lack of *mxtx2* expression (Figure 7A). At 24 hpf, 13 of 78 embryos were rescued from yolk lysis. However, all of the rescued embryos showed severe morphological defects (Figure 7A). To

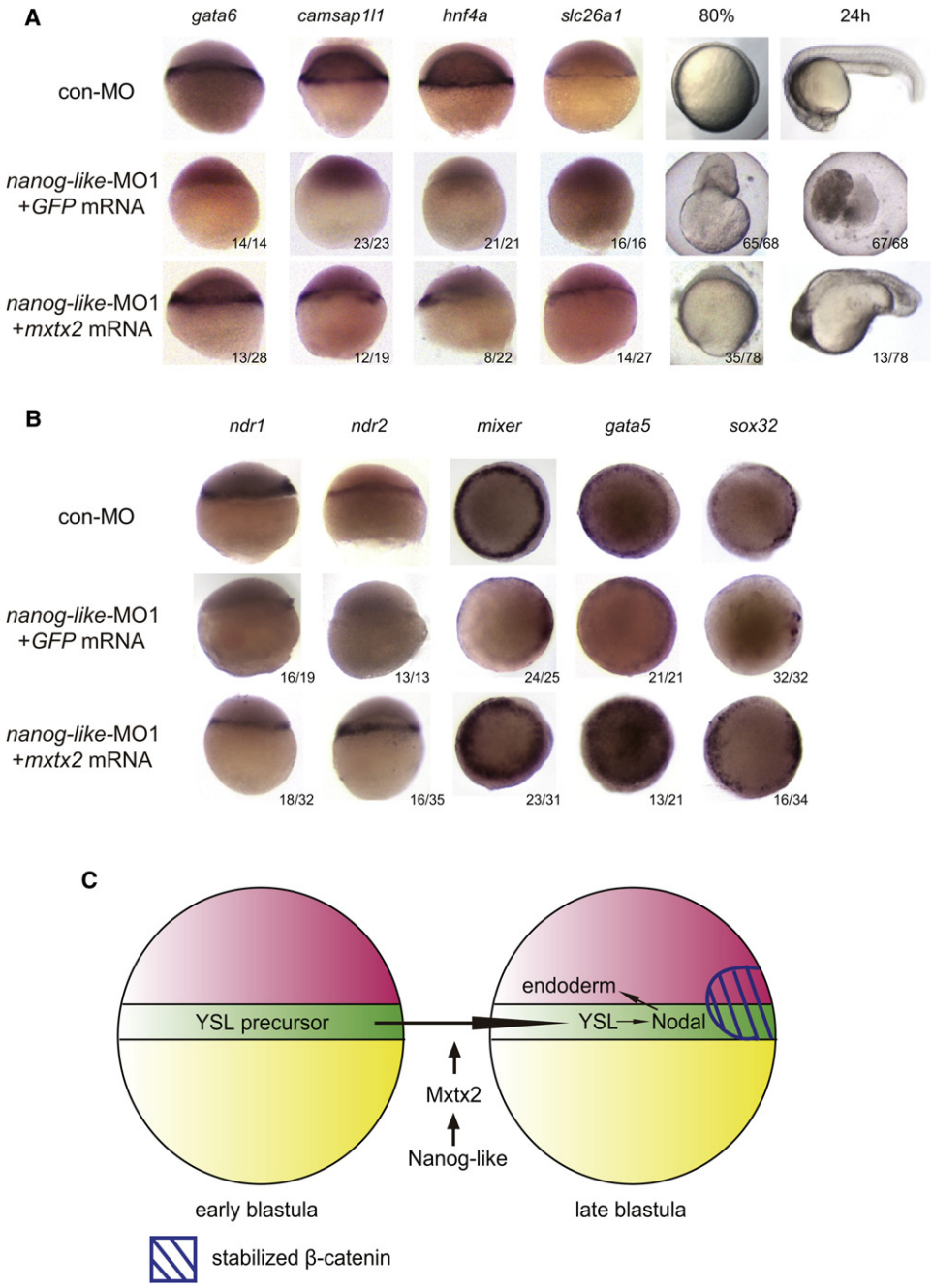

Figure 7. *mxtx2* Expression Rescues the *nanog-like* Morphant

(A) The YSL lineage was restored by *mxtx2* expression in the *nanog-like* morphant. Lateral view of embryos injected with 10 ng control morpholino (con-MO) or 10 ng *nanog-like* morpholino (*nanog-like*-MO1). *nanog-like*-MO1-injected embryos were injected with either 100 pg *GFP* mRNA or 100 pg *mxtx2* mRNA and 25 pg *GFP* mRNA at the four-cell stage. About one third of injected embryos had *GFP* expression in the YSL and were collected for further analysis. *gata6* expression was rescued in 46% (13/28) of *mxtx2*-injected embryos; *camsap1l1* expression was rescued in 63% (12/19) of *mxtx2*-injected embryos; *hnf4a* expression was rescued in 36% (8/22) of the *mxtx2*-injected embryos; and *slc26a* expression was rescued in 52% (14/27) of *mxtx2*-injected embryos. *mxtx2* expression also rescued the yolk burst phenotype in the *nanog-like* morphant. At the 80% epiboly stage, 96% (65/68) *GFP*-injected *nanog-like* morphants showed the yolk burst phenotype, and 45% (35/78) *nanog-like* morphants having *mxtx2* and *GFP* expression in the YSL showed normal epiboly progress. At 24 hpf, 99% (67/68) of *GFP*-injected *nanog-like* morphants were dead, and 17% (13/78) of *nanog-like* morphants having *mxtx2* and *GFP* expression in the YSL showed axes rescue with defective head formation and body elongation.

(B) *mxtx2* expression rescued the endoderm defect in the *nanog-like* morphant. Lateral view of embryos with dorsal side to the right. Ventrolateral *ndr1* expression was rescued in 56% (18/32) of the embryos; *ndr2* expression was rescued in 45% (16/35) of the embryos; *mixer* expression was rescued in 74% (23/31) of the embryos; *gata5* expression was rescued in 62% (13/21) of the embryos; and *sox32* expression was rescued in 47% (16/34) of the embryos.

investigate if the ventrolateral endoderm could also be rescued by Mxtx2, we examined the expression patterns of Nodal genes and endoderm genes and found that the expression patterns of both Nodals and endoderm genes were restored by *mxtx2* in *nanog-like* morphants (Figure 7B). In addition, YSL and endoderm defects in *mxtx2* morphants cannot be rescued by overexpressing *nanog-like* (data not shown). Together, these results suggest that Nanog-like induces the expression of *mxtx2*, which acts downstream of Nanog-like to establish the proper function of the YSL required for endoderm induction.

DISCUSSION

Our studies have established a role for Nanog-like during zebrafish YSL development. We propose a model in which Nanog-like regulates endoderm formation through an Mxtx2-Nodal pathway. During the early blastula stage (2.5 hpf), marginal blastomere cells collapse to form the YSL precursor. In the YSL precursor, Nanog-like directly activates Mxtx2, which, in turn, specifies the YSL lineage by directly activating the expression of YSL genes. During the late blastula stage, the YSL functions as a signaling center producing Nodal molecules for ventrolateral endoderm induction. The dorsal endoderm is induced by stabilized β-catenin-activated Nodal independent of Nanog-like (Figure 7C).

The pluripotency network described in embryonic stem cells has not been studied in the developmental ICM or in the epiblast. Zebrafish produce a large number of embryos, providing us with an opportunity to access the in vivo network. One important element in succeeding in a ChIP-Seq experiment is having a reliable antibody for the transcription factor of interest. To overcome the lack of antibodies in zebrafish studies, we developed a technique that allowed us to perform ChIP-Seq analysis utilizing embryos expressing Myc-tagged transcription factors. Using this technique, we examined the Nanog-like and Mxtx2 gene regulatory network in blastula stage zebrafish embryos. We found that Nanog-like binds to known pluripotency genes such as *pou5f1*, *sox2*, and *nanog-like*. We also found that Nanog-like bound to genes involved in extraembryonic lineage differentiation (e.g., *gata3* and *krt4* for EVL differentiation and *mxtx2* and *slc26a1* for YSL differentiation), mesoderm specification (e.g., *ntl* and *tbx3*), and cell movement (e.g., *wnt11* and *cxcr4b*), as well as to signaling genes such as *ndr1*, *bmp2b*, *fgf8a*, and *wnt8a*. The binding profile suggests that Nanog-like may play a versatile role involving many developmental processes. Another intriguing finding is that Nanog-like and Mxtx2 bound to *nanog-like* and *mxtx2* loci, suggesting potential cross-regulation and autoregulation loops between these two genes. This observation prompted us to test whether Nanog-like could rescue *mxtx2* morphants. By overexpressing *nanog-like*, we were not able to rescue the YSL and endoderm defects in *mxtx2* morphants (data not shown). This is consistent with our findings that Mxtx2 functions downstream of Nanog-like.

Mxtx2 is critical for YSL induction. The expression of *mxtx2* is highly regulated, suggested by the fact that both the high-stage Nanog-like and Mxtx2 binding sites at the *mxtx2* locus are the strongest across the entire genome. *nanog-like* is ubiquitously expressed in all blastomere cells, and its overexpression does not induce ectopic *mxtx2* expression, which suggests that it is not responsible for the spatial expression of *mxtx2*. The spatial restriction of *mxtx2* expression to the YSL may be a result of the formation of the YSL structure through collapsing of marginal cells into the yolk. One possibility is that one signaling pathway is activated in the YSL by this event, which, in turn, activates the expression of *mxtx2* in the YSL.

The YSL is unique to teleosts and has been considered an equivalent of the mouse primitive endoderm. It is interesting that Nanog is required for primitive endoderm formation, but with a distinct mechanism. Recent studies found that Nanog regulates primitive endoderm formation through a non-cell-autonomous mechanism (Frankenberg et al., 2011; Messerschmidt and Kemler, 2010). Our study suggests that, in zebrafish, Nanog-like regulates YSL formation through a cell-autonomous mechanism. While the YSL and the primitive endoderm share similar gene expression and both function as the signaling center that patterns the head mesoderm and endoderm, the regulation mechanism involving their formation is different. The fibroblast growth factor signal that is required for mouse primitive endoderm induction seems not to be involved in YSL formation (Chazaud et al., 2006; Yamanaka et al., 2010). Moreover, Gata4 and Gata6, key transcription factors in regulating primitive endoderm formation, are dispensable for YSL formation (Holtzinger and Evans, 2007; Koutsourakis et al., 1999; Peterkin et al., 2007).

Compelling evidence suggests that pluripotency factors have distinct roles in mammals and teleosts. In zebrafish, the acquisition of pluripotency by deep cells (the mouse epiblast equivalent) is independent of Nanog-like, as *nanog-like*-deficient deep cells can readily differentiate into the three germ layers (Figure 2A; data not shown). It should be noted that maternally deposited Nanog-like protein cannot be eliminated by the morpholino knockdown approach. A similar observation was made in the maternal-zygotic (MZ) *pou5f1* mutant. Pou5f1 is required for the formation of pluripotent ICM in the mouse blastocyst (Nichols et al., 1998), but the zebrafish MZ *pou5f1* mutant, lacking both maternal and zygotic expression, was still capable of differentiating into three germ layers (Lunde et al., 2004; Reim et al., 2004). Despite the findings of Schuff et al., who recently showed that zebrafish Nanog-like prevents murine embryoid body (EB) differentiation (Schuff et al., 2011), our data reveal that overexpression of zebrafish *nanog-like* does not rescue LIF dependence in murine ES cells (Figures S1D–S1F). Certain structural domains may be responsible, as zebrafish *pou5f1* does not rescue mouse *Pou5f1* mutant ES cells (Morrison and Brickman, 2006). The conservation of Nanog-like and Pou5f1 is supported by the fact that both zebrafish mutants can be rescued by their mammalian counterparts (Figures 1F and 1G) (Onichtchouk

(C) Model for endoderm and YSL induction. During early blastula development, the YSL precursor is formed by the collapse of marginal cells into the yolk cell. Acquisition of the YSL fate is mediated by Nanog-like through activation of the YSL master regulator Mxtx2. Stabilized β-catenin activates Nodal signals for endoderm induction in the dorsal region. The YSL and marginal blastomeres produce Nodal signals to induce the ventrolateral endoderm formation.

et al., 2010). However, Nanog-like's role in YSL differentiation and Pou5f1's role in endoderm differentiation do not seem to be conserved in mammals (Figures 3A and 3B) (Lunde et al., 2004; Reim et al., 2004). We speculate that the ancestors of pluripotency regulators adopted distinct functions during teleost evolution.

Our work reveals a role for Nanog-like in regulating the formation of the extraembryonic lineage, which later secretes Nodal signals to break down the pluripotency of the deep cell. Our studies suggest that the pluripotency network may have distinct roles on germ layer formation in vivo.

EXPERIMENTAL PROCEDURES

Zebrafish Maintenance

Zebrafish were maintained in accordance with animal research guidelines at Children's Hospital Boston. The wild-type embryos were collected by natural spawning from the TU strain and staged as described (Westerfield, 1995).

Morpholino and mRNA Injection

Morpholinos were obtained from Gene Tools, LLC, (*nanog-like*-MO1: 5′-CTGGCATCTTCCAGTCCGCCATTTC-3′; *nanog-like*-MO2: 5′-AGTCCGCCATTTCGCCGTTAGATAA-3′; *mxtx2*-MO: 5′-CATTGAGTATTTTGCAGCTCTCTTG-3′; control-MO: 5′-CCTCTTACCTCAGTTACAATTTATA-3′) and injected into one-cell stage embryos. Capped mRNA was generated using mMessage mMachine (Ambion) and injected into one-cell stage embryos if not specified.

Microarray Analysis

RNA was extracted by Trizol reagent (Invitrogen). We performed microarray hybridization at Roche NimbeGen (Reykjavik, Iceland) using the NimbleGen zebrafish expression array. The goldenspike package in Bioconductor/R was used to process CEL files and to identify genes with relative changes in mRNA levels between wild-type and *nanog-like* morphants. A $\log_2$ mean fold change was calculated along with a q value. Heat map was generated by Arraystar (DNASTAR).

RNase and Rhodamine Dextran Injection

Ribonuclease A (Sigma-Aldrich) was diluted in water for a final concentration of 10 μg/ml and coinjected with 4 mg/ml rhodamine dextran (Invitrogen) in the yolk of 1K-cell-stage (3 hpf) embryos. We injected 1 nl per embryo.

Blastoderm Transplants

Blastoderm transplantation was performed as described previously (Holloway et al., 2009; Yamaha et al., 2001). Briefly, 1K-cell-stage embryos were dechlorinated in agarose-coated petri dishes. Wild-type and morphant embryos were transferred to an agarose-coated petri dish with in 1X Ringers/1.6% whipped egg white. A pulled glass capillary knife and a polished glass capillary probe were used to separate the blastoderm from the yolk. Donor blastoderms were positioned onto host yolks under gentle pressure until adherent. After 5–10 min of healing, chimeric embryos were transferred to 1/3 Ringers solution for further development.

ChIP-Seq

We tagged 3′ ends of *nanog-like* and *mxtx2* coding sequences with a repeated Myc-epitope-coding sequence using the tol2kit (Harbison et al., 2004; Kwan et al., 2007). We injected 1 nl of 25ng/μl capped mRNA per embryo. For each CHIP experiment, we used 2,000 injected embryos.

Chromatin immunoprecipitation experiments were performed as previously described (Lee et al., 2006) with modifications at the crosslinking step. Injected embryos were staged and dechorionated by pronase (Roche) and washed twice with E3 embryo water. Embryos were transferred to 15-ml falcon tubes in E3 and crosslinked by the addition of 37% formaldehyde to a final concentration of 1% for 5 min at room temperature with shaking. The crosslinking was quenched by the addition of 1/20 volume 2.5 M glycine for 3 min at room temperature with shaking. Embryos were washed twice with ice-cold PBS and the pellet was flash-frozen in liquid nitrogen. Embryos were kept at −80°C until the experiments were performed. The Myc tag antibody (Abcam, ab9132) was used in the immunoprecipitation step. Detailed ChIP methods are described in the Supplemental Experimental Procedures.

The ChIP DNA samples were prepared with the Illumina/Solexa Genomic DNA kit (Illumina- IP-102-1001) and sequenced on the Illumina Genome Analyzer 1G. Detailed analysis methods are described in the Extended Experimental Procedure.

ACCESSION NUMBERS

Microarray (GSE34682) and ChIP-seq (GSE34683) data were deposited in GEO (http://www.ncbi.nlm.nih.gov/geo/) under the accession numbers indicated.

SUPPLEMENTAL INFORMATION

Supplemental Information includes five figures, three tables, Supplemental Experimental Procedures, and two movies and can be found with this article online at doi:10.1016/j.devcel.2012.01.003.

ACKNOWLEDGMENTS

This work was supported by National Institutes of Health grants 5R01HL048801-18 and 5U01HL10001-02 (L.I.Z.), R01 HG002668 (R.A.Y.), and HL056182 (T.E.). We thank I. Swinburne, J. Mullor, and R. Zhao for providing reagents; Y. Zhou, A. Chen, and L. Lawson for technical assistance; and O. Tamplin for critical appraisal of the work. L.I.Z. and G.Q.D. are Howard Hughes Medical Institute investigators. L.I.Z. is a founder and stockholder of Fate, Inc., and a scientific advisor for Stemgent.

Received: February 11, 2011
Revised: September 19, 2011
Accepted: January 11, 2012
Published online: March 12, 2012

REFERENCES

Boyer, L.A., Lee, T.I., Cole, M.F., Johnstone, S.E., Levine, S.S., Zucker, J.P., Guenther, M.G., Kumar, R.M., Murray, H.L., Jenner, R.G., et al. (2005). Core transcriptional regulatory circuitry in human embryonic stem cells. Cell *122*, 947–956.

Brown, K., Legros, S., Artus, J., Doss, M.X., Khanin, R., Hadjantonakis, A.K., and Foley, A. (2010). A comparative analysis of extra-embryonic endoderm cell lines. PLoS ONE *5*, e12016.

Bruce, A.E.E., Howley, C., Dixon Fox, M., and Ho, R.K. (2005). T-box gene eomesodermin and the homeobox-containing Mix/Bix gene mtx2 regulate epiboly movements in the zebrafish. Dev. Dyn. *233*, 105–114.

Chambers, I., Colby, D., Robertson, M., Nichols, J., Lee, S., Tweedie, S., and Smith, A. (2003). Functional expression cloning of Nanog, a pluripotency sustaining factor in embryonic stem cells. Cell *113*, 643–655.

Chazaud, C., Yamanaka, Y., Pawson, T., and Rossant, J. (2006). Early lineage segregation between epiblast and primitive endoderm in mouse blastocysts through the Grb2-MAPK pathway. Dev. Cell *10*, 615–624.

Chen, S., and Kimelman, D. (2000). The role of the yolk syncytial layer in germ layer patterning in zebrafish. Development *127*, 4681–4689.

Chen, X., Xu, H., Yuan, P., Fang, F., Huss, M., Vega, V.B., Wong, E., Orlov, Y.L., Zhang, W., Jiang, J., et al. (2008). Integration of external signaling pathways with the core transcriptional network in embryonic stem cells. Cell *133*, 1106–1117.

Cheng, J.C., Miller, A.L., and Webb, S.E. (2004). Organization and function of microfilaments during late epiboly in zebrafish embryos. Dev. Dyn. *231*, 313–323.

Cole, M.F., Johnstone, S.E., Newman, J.J., Kagey, M.H., and Young, R.A. (2008). Tcf3 is an integral component of the core regulatory circuitry of embryonic stem cells. Genes Dev. *22*, 746–755.

Dickmeis, T., Mourrain, P., Saint-Etienne, L., Fischer, N., Aanstad, P., Clark, M., Strähle, U., and Rosa, F. (2001). A crucial component of the endoderm formation pathway, CASANOVA, is encoded by a novel sox-related gene. Genes Dev. *15*, 1487–1492.

Dixon, J.E., Allegrucci, C., Redwood, C., Kump, K., Bian, Y., Chatfield, J., Chen, Y.H., Sottile, V., Voss, S.R., Alberio, R., and Johnson, A.D. (2010). Axolotl Nanog activity in mouse embryonic stem cells demonstrates that ground state pluripotency is conserved from urodele amphibians to mammals. Development *137*, 2973–2980.

Fan, X., Hagos, E.G., Xu, B., Sias, C., Kawakami, K., Burdine, R.D., and Dougan, S.T. (2007). Nodal signals mediate interactions between the extra-embryonic and embryonic tissues in zebrafish. Dev. Biol. *310*, 363–378.

Feldman, B., Gates, M.A., Egan, E.S., Dougan, S.T., Rennebeck, G., Sirotkin, H.I., Schier, A.F., and Talbot, W.S. (1998). Zebrafish organizer development and germ-layer formation require nodal-related signals. Nature *395*, 181–185.

Frankenberg, S., Gerbe, F., Bessonnard, S., Belville, C., Pouchin, P., Bardot, O., and Chazaud, C. (2011). Primitive Endoderm Differentiates via a Three-Step Mechanism Involving Nanog and RTK Signaling. Dev. Cell *21*, 1005–1013.

Gritsman, K., Zhang, J., Cheng, S., Heckscher, E., Talbot, W.S., and Schier, A.F. (1999). The EGF-CFC protein one-eyed pinhead is essential for nodal signaling. Cell *97*, 121–132.

Harbison, C.T., Gordon, D.B., Lee, T.I., Rinaldi, N.J., Macisaac, K.D., Danford, T.W., Hannett, N.M., Tagne, J.B., Reynolds, D.B., Yoo, J., et al. (2004). Transcriptional regulatory code of a eukaryotic genome. Nature *431*, 99–104.

Ho, C.Y., Houart, C., Wilson, S.W., and Stainier, D.Y. (1999). A role for the extraembryonic yolk syncytial layer in patterning the zebrafish embryo suggested by properties of the hex gene. Curr. Biol. *9*, 1131–1134.

Holloway, B.A., Gomez de la Torre Canny, S., Ye, Y., Slusarski, D.C., Freisinger, C.M., Dosch, R., Chou, M.M., Wagner, D.S., and Mullins, M.C. (2009). A novel role for MAPKAPK2 in morphogenesis during zebrafish development. PLoS Genet. *5*, e1000413.

Holtzinger, A., and Evans, T. (2007). Gata5 and Gata6 are functionally redundant in zebrafish for specification of cardiomyocytes. Dev. Biol. *312*, 613–622.

Hong, S.-K., Levin, C.S., Brown, J.L., Wan, H., Sherman, B.T., Huang, D.W., Lempicki, R.A., and Feldman, B. (2010). Pre-gastrula expression of zebrafish extraembryonic genes. BMC Dev. Biol. *10*, 42.

Hong, S.-K., Jang, M.K., Brown, J.L., McBride, A.A., and Feldman, B. (2011). Embryonic mesoderm and endoderm induction requires the actions of non-embryonic Nodal-related ligands and Mxtx2. Development *138*, 787–795.

Kane, D.A., Warga, R.M., and Kimmel, C.B. (1992). Mitotic domains in the early embryo of the zebrafish. Nature *360*, 735–737.

Kikuchi, Y., Trinh, L.A., Reiter, J.F., Alexander, J., Yelon, D., and Stainier, D.Y. (2000). The zebrafish bonnie and clyde gene encodes a Mix family homeodomain protein that regulates the generation of endodermal precursors. Genes Dev. *14*, 1279–1289.

Kikuchi, Y., Agathon, A., Alexander, J., Thisse, C., Waldron, S., Yelon, D., Thisse, B., and Stainier, D.Y. (2001). casanova encodes a novel Sox-related protein necessary and sufficient for early endoderm formation in zebrafish. Genes Dev. *15*, 1493–1505.

Kimmel, C.B., and Law, R.D. (1985a). Cell lineage of zebrafish blastomeres. I. Cleavage pattern and cytoplasmic bridges between cells. Dev. Biol. *108*, 78–85.

Kimmel, C.B., and Law, R.D. (1985b). Cell lineage of zebrafish blastomeres. II. Formation of the yolk syncytial layer. Dev. Biol. *108*, 86–93.

Köppen, M., Fernández, B.G., Carvalho, L., Jacinto, A., and Heisenberg, C.P. (2006). Coordinated cell-shape changes control epithelial movement in zebrafish and Drosophila. Development *133*, 2671–2681.

Koutsourakis, M., Langeveld, A., Patient, R., Beddington, R., and Grosveld, F. (1999). The transcription factor GATA6 is essential for early extraembryonic development. Development *126*, 723–732.

Kwan, K.M., Fujimoto, E., Grabher, C., Mangum, B.D., Hardy, M.E., Campbell, D.S., Parant, J.M., Yost, H.J., Kanki, J.P., and Chien, C.B. (2007). The Tol2kit: a multisite gateway-based construction kit for Tol2 transposon transgenesis constructs. Dev. Dyn. *236*, 3088–3099.

Lee, T.I., Johnstone, S.E., and Young, R.A. (2006). Chromatin immunoprecipitation and microarray-based analysis of protein location. Nat. Protoc. *1*, 729–748.

Loh, Y.H., Wu, Q., Chew, J.L., Vega, V.B., Zhang, W., Chen, X., Bourque, G., George, J., Leong, B., Liu, J., et al. (2006). The Oct4 and Nanog transcription network regulates pluripotency in mouse embryonic stem cells. Nat. Genet. *38*, 431–440.

Lunde, K., Belting, H.G., and Driever, W. (2004). Zebrafish pou5f1/pou2, homolog of mammalian Oct4, functions in the endoderm specification cascade. Curr. Biol. *14*, 48–55.

Marson, A., Levine, S.S., Cole, M.F., Frampton, G.M., Brambrink, T., Johnstone, S., Guenther, M.G., Johnston, W.K., Wernig, M., Newman, J., et al. (2008). Connecting microRNA genes to the core transcriptional regulatory circuitry of embryonic stem cells. Cell *134*, 521–533.

Messerschmidt, D.M., and Kemler, R. (2010). Nanog is required for primitive endoderm formation through a non-cell autonomous mechanism. Dev. Biol. *344*, 129–137.

Mitsui, K., Tokuzawa, Y., Itoh, H., Segawa, K., Murakami, M., Takahashi, K., Maruyama, M., Maeda, M., and Yamanaka, S. (2003). The homeoprotein Nanog is required for maintenance of pluripotency in mouse epiblast and ES cells. Cell *113*, 631–642.

Mizuno, T., Yamaha, E., Wakahara, M., Kuroiwa, A., and Takeda, H. (1996). Mesoderm induction in zebrafish. Nature *383*, 131–132.

Morrison, G.M., and Brickman, J.M. (2006). Conserved roles for Oct4 homologues in maintaining multipotency during early vertebrate development. Development *133*, 2011–2022.

Nichols, J., Zevnik, B., Anastassiadis, K., Niwa, H., Klewe-Nebenius, D., Chambers, I., Schöler, H., and Smith, A. (1998). Formation of pluripotent stem cells in the mammalian embryo depends on the POU transcription factor Oct4. Cell *95*, 379–391.

Ober, E.A., and Schulte-Merker, S. (1999). Signals from the yolk cell induce mesoderm, neuroectoderm, the trunk organizer, and the notochord in zebrafish. Dev. Biol. *215*, 167–181.

Onichtchouk, D., Geier, F., Polok, B., Messerschmidt, D.M., Mössner, R., Wendik, B., Song, S., Taylor, V., Timmer, J., and Driever, W. (2010). Zebrafish Pou5f1-dependent transcriptional networks in temporal control of early development. Mol. Syst. Biol. *6*, 354.

Peterkin, T., Gibson, A., and Patient, R. (2007). Redundancy and evolution of GATA factor requirements in development of the myocardium. Dev. Biol. *311*, 623–635.

Poulain, M., and Lepage, T. (2002). Mezzo, a paired-like homeobox protein is an immediate target of Nodal signalling and regulates endoderm specification in zebrafish. Development *129*, 4901–4914.

Reim, G., Mizoguchi, T., Stainier, D.Y., Kikuchi, Y., and Brand, M. (2004). The POU domain protein spg (pou2/Oct4) is essential for endoderm formation in cooperation with the HMG domain protein casanova. Dev. Cell *6*, 91–101.

Reiter, J.F., Alexander, J., Rodaway, A., Yelon, D., Patient, R., Holder, N., and Stainier, D.Y. (1999). Gata5 is required for the development of the heart and endoderm in zebrafish. Genes Dev. *13*, 2983–2995.

Rodaway, A., Takeda, H., Koshida, S., Broadbent, J., Price, B., Smith, J.C., Patient, R., and Holder, N. (1999). Induction of the mesendoderm in the zebrafish germ ring by yolk cell-derived TGF-beta family signals and discrimination of mesoderm and endoderm by FGF. Development *126*, 3067–3078.

Schier, A.F., Neuhauss, S.C., Helde, K.A., Talbot, W.S., and Driever, W. (1997). The one-eyed pinhead gene functions in mesoderm and endoderm formation in zebrafish and interacts with no tail. Development *124*, 327–342.

Schuff, M., Siegel, D., Philipp, M., Bundschu, K., Heymann, N., Donow, C., and Knöchel, W. (2011). Characterization of Danio rerio Nanog and Functional Comparison to Xenopus Vents. Stem Cells Dev., in press. Published online October 3, 2011. 10.1089/scd.2011.0285.

Silva, J., Nichols, J., Theunissen, T.W., Guo, G., van Oosten, A.L., Barrandon, O., Wray, J., Yamanaka, S., Chambers, I., and Smith, A. (2009). Nanog is the gateway to the pluripotent ground state. Cell *138*, 722–737.

Solnica-Krezel, L., and Driever, W. (1994). Microtubule arrays of the zebrafish yolk cell: organization and function during epiboly. Development *120*, 2443–2455.

Sprague, J., Bayraktaroglu, L., Clements, D., Conlin, T., Fashena, D., Frazer, K., Haendel, M., Howe, D.G., Mani, P., Ramachandran, S., et al. (2006). The Zebrafish Information Network: the zebrafish model organism database. Nucleic Acids Res. *34* (Database issue), D581–D585.

Strähle, U., and Jesuthasan, S. (1993). Ultraviolet irradiation impairs epiboly in zebrafish embryos: evidence for a microtubule-dependent mechanism of epiboly. Development *119*, 909–919.

Varlet, I., Collignon, J., and Robertson, E.J. (1997). nodal expression in the primitive endoderm is required for specification of the anterior axis during mouse gastrulation. Development *124*, 1033–1044.

Wang, J., Rao, S., Chu, J., Shen, X., Levasseur, D.N., Theunissen, T.W., and Orkin, S.H. (2006). A protein interaction network for pluripotency of embryonic stem cells. Nature *444*, 364–368.

Wang, J., Levasseur, D.N., and Orkin, S.H. (2008). Requirement of Nanog dimerization for stem cell self-renewal and pluripotency. Proc. Natl. Acad. Sci. USA *105*, 6326–6331.

Westerfield, M. (1995). The Zebrafish Book (Eugene, OR: University of Oregon Press).

Wilkins, S.J., Yoong, S., Verkade, H., Mizoguchi, T., Plowman, S.J., Hancock, J.F., Kikuchi, Y., Heath, J.K., and Perkins, A.C. (2008). Mtx2 directs zebrafish morphogenetic movements during epiboly by regulating microfilament formation. Dev. Biol. *314*, 12–22.

Yamaha, E., Kazama-Wakabayashi, M., Otani, S., Fujimoto, T., and Arai, K. (2001). Germ-line chimera by lower-part blastoderm transplantation between diploid goldfish and triploid crucian carp. Genetica *111*, 227–236.

Yamanaka, Y., Lanner, F., and Rossant, J. (2010). FGF signal-dependent segregation of primitive endoderm and epiblast in the mouse blastocyst. Development *137*, 715–724.